Scanning Microscopy

Volume 7 | Number 2 Article 13

6-9-1993

Analysis of Synthetic DNAs and DNA-Protamine Complexes with the Scanning Tunneling Microscope

Michael J. Allen
Lawrence Livermore National Laboratory

Robert J. Tench
Lawrence Livermore National Laboratory

Joe A. Mazrimas
Lawrence Livermore National Laboratory

Mehdi Balooch
Lawrence Livermore National Laboratory

Wigbert J. Siekhaus
Lawrence Livermore National Laboratory

See next page for additional authors

Follow this and additional works at: https://digitalcommons.usu.edu/microscopy

 Part of the Biology Commons

Recommended Citation

Allen, Michael J.; Tench, Robert J.; Mazrimas, Joe A.; Balooch, Mehdi; Siekhaus, Wigbert J.; and Balhorn, Rod (1993) "Analysis of Synthetic DNAs and DNA-Protamine Complexes with the Scanning Tunneling Microscope," *Scanning Microscopy*: Vol. 7 : No. 2 , Article 13.
Available at: https://digitalcommons.usu.edu/microscopy/vol7/iss2/13

This Article is brought to you for free and open access by the Western Dairy Center at DigitalCommons@USU. It has been accepted for inclusion in Scanning Microscopy by an authorized administrator of DigitalCommons@USU. For more information, please contact digitalcommons@usu.edu.

Analysis of Synthetic DNAs and DNA-Protamine Complexes with the Scanning Tunneling Microscope

Authors

Michael J. Allen, Robert J. Tench, Joe A. Mazrimas, Mehdi Balooch, Wigbert J. Siekhaus, and Rod Balhorn

This article is available in Scanning Microscopy: https://digitalcommons.usu.edu/microscopy/vol7/iss2/13

Scanning Microscopy, Vol. 7, No. 2, 1993 (Pages 563-576)
Scanning Microscopy International, Chicago (AMF O'Hare), IL 60666 USA

0891-7035/93$5.00+.00

ANALYSIS OF SYNTHETIC DNAs AND DNA-PROTAMINE COMPLEXES WITH THE SCANNING TUNNELING MICROSCOPE

Michael J. Allen[1], Robert J. Tench[2], Joe A. Mazrimas[1], Mehdi Balooch[3], Wigbert J. Siekhaus[3] and Rod Balhorn[1]

[1]Biomedical Sciences Division, [2]Department of Applied Sciences, [3]Department of Chemistry and Materials Science
Lawrence Livermore National Laboratory
Livermore, CA 94550

(Received for publication April 13, 1992, and in revised form June 9, 1993)

Abstract

Three duplex DNAs 22, 47, and 100 base-pairs in length have been imaged with the scanning tunneling microscope (STM) after deposition on highly oriented pyrolytic graphite (HOPG). Images of the 47 base-pair (bp) molecules are resolved sufficiently to identify the two phosphodiester strands, the direction of helical coiling (this molecule contains three turns of left-handed helix), and single-stranded ends. Length measurements indicate that all three DNA sequences have adopted an "A-like" conformation. DNA-protamine complexes were also prepared and imaged under similar conditions. Length measurements of the complexes demonstrate that the binding of bull protamine 1 to the 47-mer stabilizes the DNA in a B conformation and prevents the B to A transition that has been shown to occur as the DNA molecules dehydrate on the surface. Measurements of the diameter of the complex (3 nm) were also obtained and were found to be only slightly larger than the DNA molecule. This observation is consistent with the binding of the protamine molecule inside one of the grooves.

Key Words: Scanning tunneling microscopy (STM), DNA, protamine, DNA conformation, B conformation, oligonucleotides.

*Address for Correspondence:
Rod Balhorn
Biomedical Sciences Division, L-452
Lawrence Livermore National Laboratory
Livermore, CA 94550
Telephone Number: (510) 422-6284
FAX Number: (510) 422-2282

Introduction

Scanning tunneling microscopy (Binnig and Rohrer, 1982, 1985) has been used successfully to obtain images of a variety of surfaces and molecular structures at or near atomic resolution. These include semiconductor and metal surfaces (Hansma and Tersoff, 1987), small organic molecules such as benzene (Ohtani *et al.*, 1988) and phthalates (Foster *et al.*, 1988), n-alkylcyanobiphenyl (Smith *et al.*, 1989, 1990), copper phthalocyanine (Gimzewski *et al.*, 1987), conducting polymers (Sleator and Tycko, 1988; Yang *et al.*, 1990), films of liquid crystals (Foster and Frommer, 1988; Spong *et al.*, 1989), and Langmuir-Blodgett films (Eng *et al.*, 1988; Lang *et al.*, 1988). Within the last several years, numerous laboratories have attempted to apply this new microscopy to the analysis of biologically relevant structures. Images have been obtained of bacteriophage virus particles (Baro *et al.*, 1985, Keller *et al.*, 1990), chloroplasts (Mainsbridge and Thundat, 1991), bacterial flagella (Nakagiri *et al.*, 1991), untreated (Gaczynska *et al.*, 1991) and freeze-fractured metal replicas of biomembranes (Hansma *et al.*, 1988; Zasadzinski *et al.*, 1988), cell walls and surfaces (Beveridge *et al.*, 1990; Blackford *et al.*, 1991; Dai *et al.*, 1991; Ito *et al.*, 1991), nuclear envelopes (Stemmer *et al.*, 1991), cyclodextrin (Miles *et al.*, 1990), peptides (Zheng *et al.*, 1991) and small proteins (Edstrom *et al.*, 1989; Feng *et al.*, 1989; Haggerty *et al.*, 1991; Miles *et al.*, 1991; Yeung *et al.*, 1991), DNA-protein complexes (Amrein *et al.*, 1988; Lu *et al.*, 1991), collagen (Zhu *et al.*, 1991), and microtubules (Hameroff *et al.*, 1990). Other studies have provided images of RNA (Lesniewska *et al.*, 1991) and single and double-stranded DNA deposited on gold and graphite at various levels of resolution (Allison *et al.*, 1990; Arscott *et al.*, 1989; Barris *et al.*, 1988; Beebe Jr. *et al.*, 1989; Bendixen *et al.*, 1990; Cricenti *et al.*, 1989, 1991; Driscoll *et al.*, 1990; Dunlap and Bustamante, 1990; Keller *et al.*, 1989; Kim and Lieber, 1991; Lee *et al.*, 1989; Li *et al.*, 1991; Lindsay and Barris, 1988; Lindsay *et al.*, 1989; Travaglini *et al.*, 1987; Youngquist *et al.*, 1991) as well as the individual bases of DNA (Allen *et al.*, 1991; Heckl *et al.*, 1991).

22-MER

```
5'-TGCAGTTCGTTCGAATGTACAA-3'
   ACGTCAAGCAAGCTTACATGTT
```

47-MER

```
5'-AATTCTTTAAAGATCGATATCGCGGTACCCGGGCCCGTTAACAGCTGAGCG-3'
       GAAATTTCTAGCTATAGCGCCATGGGCCCGGGCAATTGTCGACTCGCTTAA
```

100-MER

```
5'-AATTCTTTAAAGATCGATATCGCGGTACGCGGCGCCGTTAACAGCTGAGCGATATCTTGCGTGACTATCCGAATAGTAGCGCCTACTTACGGTTAACAGC-3'
   TTAAGAAATTTCTAGCTATAGCGCCATGCGCCGCGGCAATTGTCGACTCGCTATAGAACGCACTGATAGGCTTATCATCGCGGATGAATGCCAATTGTCG
```

Figure 1. Base sequences of the 22-bp, 47-bp and 100-bp synthetic DNAs imaged with the STM. The complimentary strands were synthesized using an Applied Biosystems 380B DNA Synthesizer, annealed, and repurified by HPLC chromatography.

These more recent studies are promising because they demonstrate that both proteins and DNA are sufficiently conductive to be imaged with the STM and that the STM can be used to obtain useful information about biologically relevant macromolecular structures. Other studies of untreated graphite have indicated, however, that a wide variety of structural features are already present on the surface of the graphite. Carbon steps, disrupted flakes of graphite, and other surface defects or contaminants are often linear and display repeating features similar to those expected for DNA (Chang and Bard, 1991; Clemmer and Beebe, 1991; Salmeron *et al.*, 1990). Reactions of the surface with aqueous reagents also complicate analyses by altering the appearance of its lattice. Consequently, considerable effort must be expended to prove that the structures being imaged are really the molecules of interest.

To facilitate future analyses of DNA-protein complexes with the STM, we have imaged three synthetic double-stranded DNAs deposited on HOPG using a voltage pulse. Both unique structural features (such as single-stranded ends) and the expected lengths of the DNAs have been used to discriminate between DNA molecules and surface or tip contaminants. A complex between bull protamine 1 and the 47-mer was also produced *in vitro* and imaged at high resolution. Length measurements of the free DNA and protamine-DNA complex have been obtained which demonstrate that free DNA molecules imaged on the surface of graphite in air adopt an A conformation. In contrast, similar measurements of the complex show that the binding of the arginine-rich protamine 1 molecule to DNA prevents the normal B to A conformational transition that occurs in DNA at low humidity.

Materials and Methods

Benzylalkonium chloride (BAC) was purchased from Sigma Chemical Co. (St. Louis, MO). The HOPG used in this study was obtained as a gift from A.W. Moore (Union Carbide Corp., Parma Technical Center, Parma, OH).

Preparation of synthetic DNAs

The oligonucleotides were synthesized using an Applied Biosystems 380B Synthesizer (Foster City, CA) and subsequently purified by high performance liquid chromatography (HPLC) without removing the dimethoxytrityl (DMT) group. The chromatography was performed using two Beckmann model 110A pumps, a model V4 ISCO detector (260 nm), and a model 420 system controller. The purification column was a 200 x 7.5 mm column packed with a silica based 5 μm C8 matrix of 30 nm pore size (W-Porex 5 C8; Phenomenex, Rancho Palos Verdes, CA). The aqueous buffer was 0.1 M triethylammonium acetate, pH 7 (A buffer) and the organic solvent was aqueous 50% acetonitrile (B buffer). The oligonucleotides were purified using a linear gradient of 7.5% to 20% acetonitrile (over a 25 minute period) and lyophilized. The DMT group was removed by 80% glacial acetic acid in water and the DNA was repurified on a Sep-Pak-C18 cartridge (Waters, Milford, MA).

Complimentary oligonucleotides were annealed in 0.1 M tris buffer, pH 7.6, by first heating them to 95°C for 5 minutes and then allowing the water bath to slowly cool to 50°C over one hour. The structures were further stabilized by maintaining the temperature at 50°C for four more hours. After storage overnight at 4°C, the duplex was purified from single-strands by injecting it into a 250 x 7.5 mm PRP-1 column (Hamilton, Reno, NV). Using a linear gradient (20 minutes) from 5% to 13.5% acetonitrile, two major peaks were obtained: the early eluting single-strands and a small amount of duplex DNA. The duplex was collected and carefully lyophilized.

Deposition of DNA molecules onto graphite and imaging with the STM

Two slightly different methods were used to deposit the DNA molecules onto HOPG. One method involved touching a freshly cleaved graphite surface to a droplet containing DNA (0.13 μg/ml in 10 mM NaCl, pH 7) and BAC (40 μg/ml in 50% formamide), rinsing the surface in distilled water, and wicking it dry. The surface was then scanned several times, pulsed at -4 volts for 10 microseconds, and scanned immediately following the pulse. In the other method, the BAC-DNA complex was transferred to the tunneling tip by dipping

the end of the Pt/Rh tip into the droplet. The DNA molecules were deposited onto the graphite surface by applying the same -4 volt pulse to the tunneling gap and the surface was immediately imaged. Both methods gave similar results.

The instrument used to produce these images was a 5 cm double-tube, kinetic/inertial approach STM constructed at Lawrence Livermore National Laboratory (LLNL). Hand cut Pt/Rh tips were used for imaging. All of the images were taken in air in a constant current/ topographical mode and have been median and smooth filtered to increase clarity. Slightly different bias voltages and tunneling currents were used for each sample (see figure legends).

Isolation of protamine and preparation of the DNA-protamine complex

Bull protamine 1 was isolated from bull sperm (American Breeders Service, DeForest, WI) and purified by HPLC on a Nucleosil RP-C18 column using a linear acetonitrile gradient as described previously (Mazrimas *et al.*, 1986). The protein was analyzed for purity by electrophoresis in acid-urea gels (Balhorn *et al.*, 1977).

Protamine was dissolved in distilled water at a concentration of 1.3 mg/ml and the 47-mer was dissolved in 10 mM sodium chloride at a concentration of 1.3 mg/ml. A single 5 μl drop of the protamine solution was applied to a freshly cleaved surface of HOPG and allowed to air dry. Immediately before imaging, a 0.1 μl drop of DNA was added to the same spot and the sample was again allowed to dry. The surface was subsequently rinsed with distilled water to remove the salt and excess, uncomplexed protamine.

Results

STM images were obtained in the topographical mode for each of the three synthetic double-stranded DNAs shown in Figure 1. Groups or arrays of the molecules were deposited by the voltage pulse onto the surface of graphite within a 100 nm radius around the tip. All of the molecules within these arrays were observed to be oriented non-radially with respect to the tip (Figure 2). Occasionally, however, a large amount of unidentifiable material would be deposited directly beneath the tip and individual, unoriented molecules would be observed nearby. The most highly resolved images were obtained of these molecules. Each of the molecules were scanned at high resolution and their lengths, widths, and helical periodicities were measured.

The images of the shortest DNAs, the 22-mers, were variable in appearance and generally featureless (Figure 3). Only occasionally could features be detected that suggested the presence of helical coiling. The surfaces were often smooth and none of the molecules displayed a measurable helical periodicity. The average length of these molecules was determined to be 5.5 $\pm$ 0.29 nm (n = 8). Images of the 47-mer and 100-mer, on the other hand, revealed knobby, filamentous features

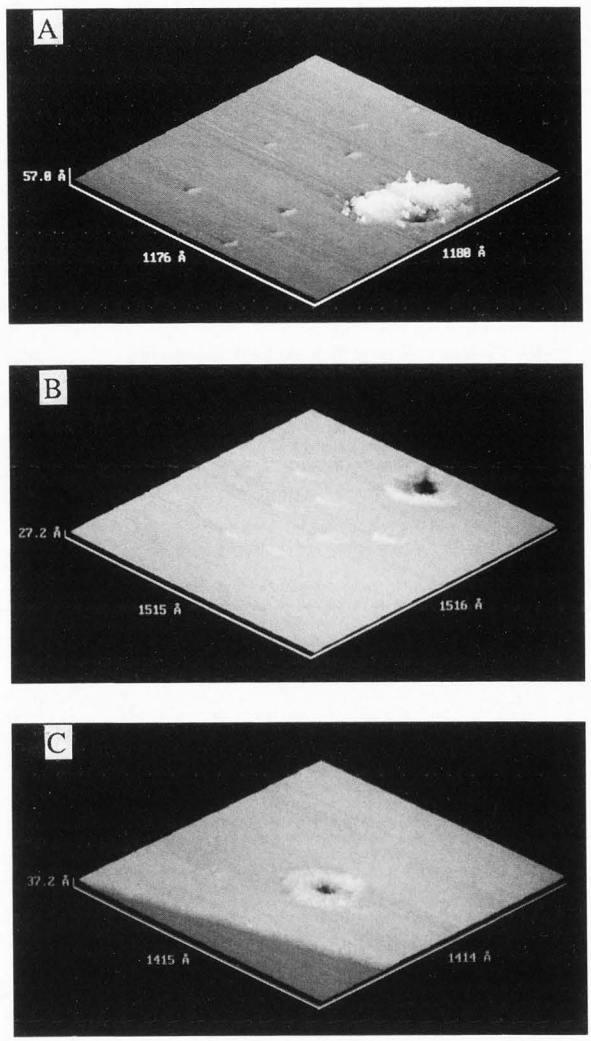

Figure 2. Low resolution scans of pulse-deposited synthetic DNAs on graphite showing their location relative to the central pit/mound of material. **A.** 22-mer. **B.** 100-mer. **C.** Control (buffer and BAC without DNA).

that corresponded to the helical coiling of the two phosphodiester strands. The 47-bp sequences (Figure 4) showed 4-5 helical turns and an average molecular length of 11.6 $\pm$ 0.29 nm (n = 8). Measurements performed on one exceptionally high quality image (the image in Figure 4B has been median and smooth filtered; a raw image of the same 47-mer is shown in Figure 4C as an example of an unfiltered image) revealed an average helical periodicity of 2.4 nm and a molecular width of 2.4 nm. Images of the 100-bp DNAs (Figure 5) revealed 6-7 helical turns immediately followed by an alteration in coiling that made it difficult to assign or identify the structure at the remaining end. Length measurements of the 100-mer DNA average 21.5 $\pm$ 1.39 nm (n = 8) with an average periodicity of 2.5 nm (over 3 measurable periods).

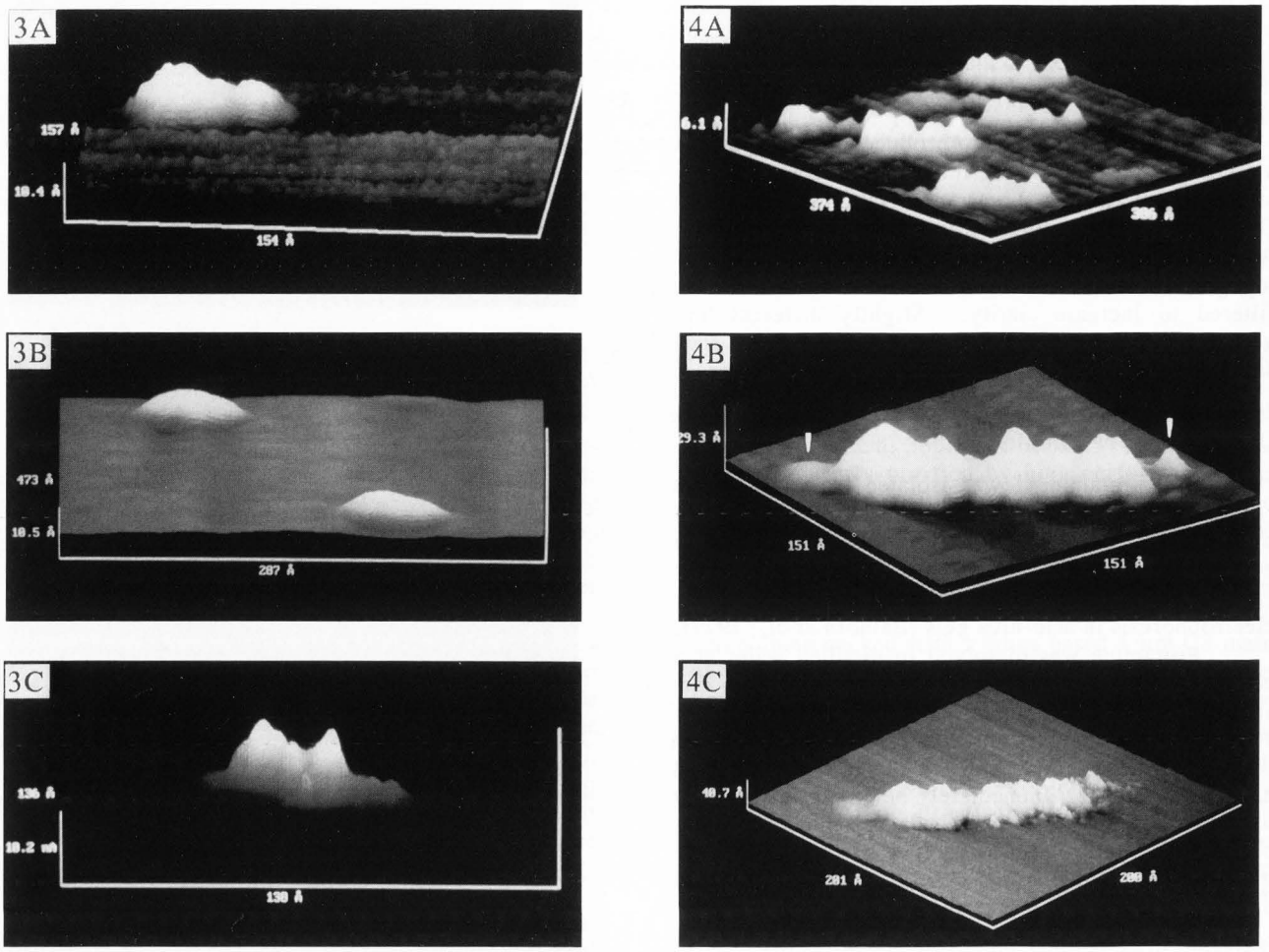

Figure 3. STM images of 22-bp DNA molecules on HOPG. A freshly cleaved HOPG surface was touched to a droplet containing DNA (0.13 μg/ml in 10 mM NaCl pH 7) and BAC (40 μg/ml in 50% formamide), quickly rinsed in distilled H_2O and wicked dry. The surface was then scanned several times, pulsed at -4 volts for 10 microseconds, and scanned again immediately following the pulse. DNA molecules were only found in post-pulse scans. The instrument used to produce these images was a 5 cm double-tube, kinetic/inertial approach STM constructed at LLNL. Hand cut Pt-Rh tips were used for imaging. All of the images presented were taken in a constant current/topographical mode and have been median and smooth filtered to increase clarity. Bias -194 mV. Tunneling current 0.94 nA.

Figure 4. STM images of 47-bp DNA molecules on HOPG. The DNA samples were prepared and deposited onto graphite as described in Figure 3. **A**. Several 47-bp DNA molecules on HOPG imaged after a 10 microsecond pulse. Many oligomers were found near a large mound of deposited material. Helical coiling and other structural features are not well defined. Bias -195 mV. Tunneling current 0.54 nA. **B**. Higher resolution image of another 47-mer with arrows pointing out the four base, single-stranded ends. **C**. Unfiltered image of the same DNA shown in B.

Figure 5. 100-bp DNA molecules pulse-deposited on HOPG following direct application of DNA to the STM tip. **A**. This molecule was found near a mound of material deposited by the tip onto the surface [DNA (2 μg/ ml in 50 mM ammonium acetate, pH 7), BAC (40 μg/ml in 60% formamide)]. Pulse amplitude was -2.7 volts with a width of 10 microseconds. The structure (20.1 nm in length) shows a periodic coiling pattern but the individual phosphodiester strands are not visible. Bias -188 mV. Tunneling current 0.61 nA. **B**. The helical coiling pattern in this molecule is visible as are the individual phosphodiester strands [DNA (0.2 mg/ml in 0.1 M ammonium acetate pH 7), BAC (1 mg/ml in 50% formamide)]. Pulse strength was -3.5 V for 10 microseconds. Here, the epicenter consisted of a small amount of deposited material in which this individual molecule could be identified. **C**. Zoomed image of the molecule in Figure 4B showing the major and minor grooves of seven of the helical turns. Total length is 21.2 nm. Bias -176 mV. Tunneling current 0.46 nA.

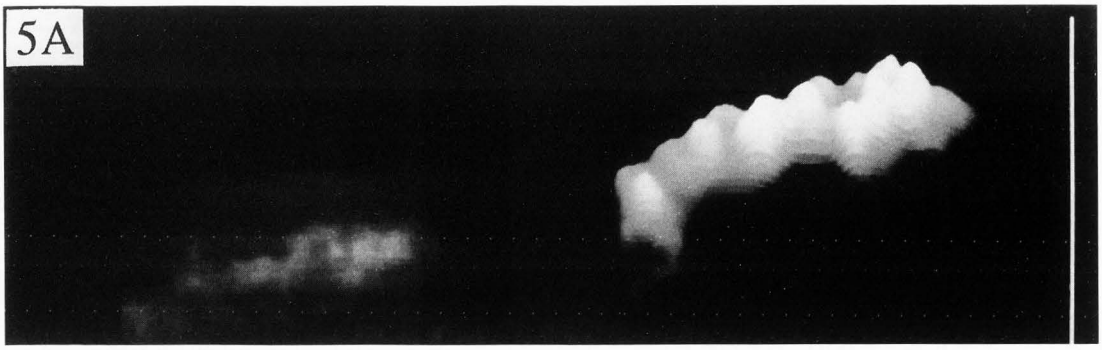
5A

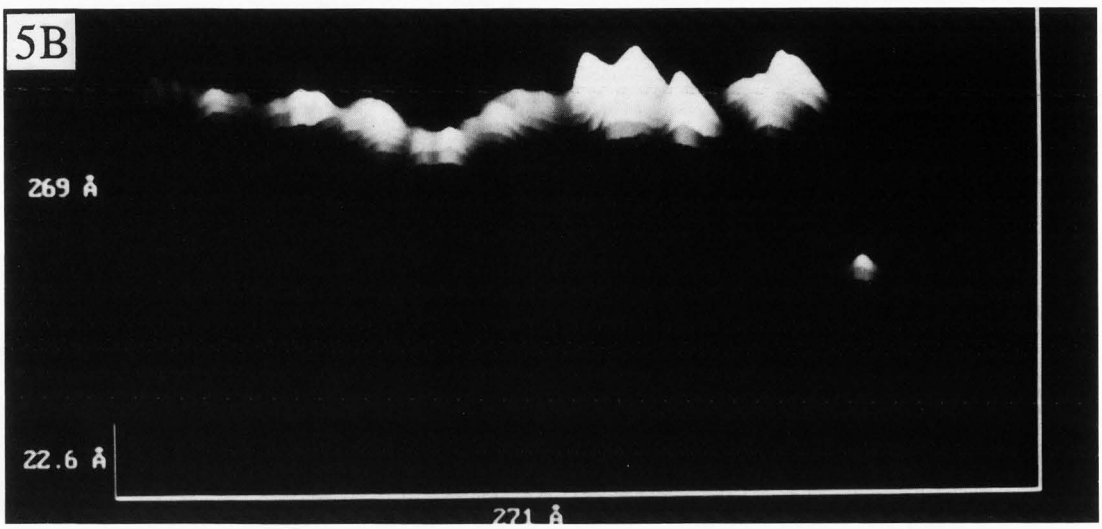
5B
269 Å
22.6 Å
271 Å

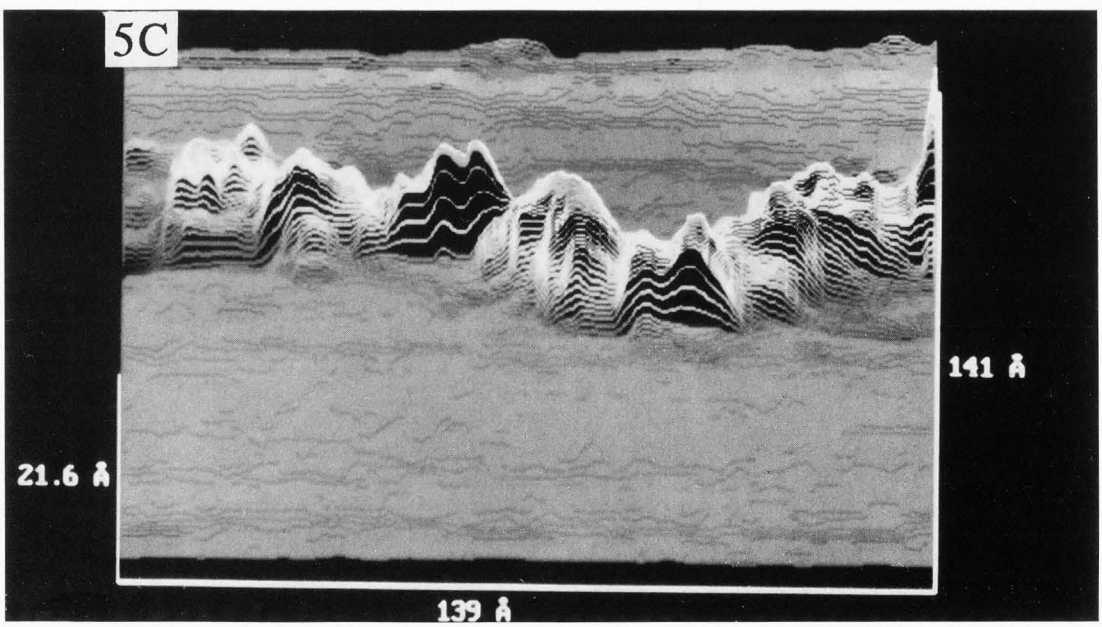
5C
141 Å
21.6 Å
139 Å

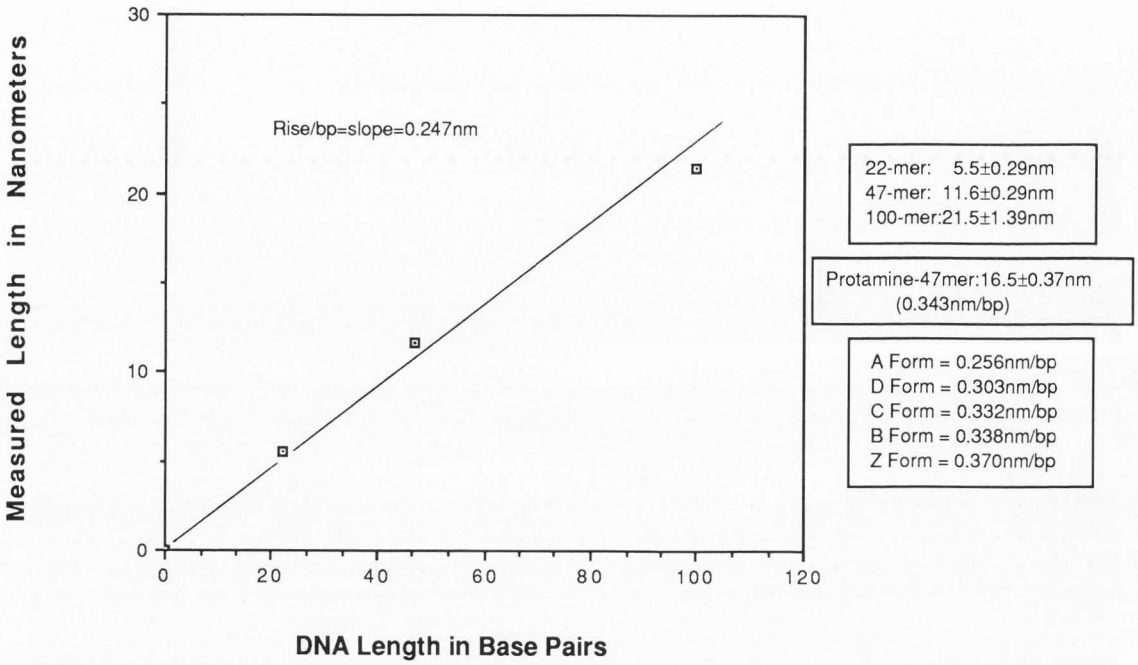

Figure 6. Measured lengths of synthetic DNAs and the 47-bp DNA-protamine complex. Multiple sample preparations were made for each oligo and the controls. The lengths of the individual structures used to provide the statistics were obtained from two different experiments with 22-mers, four experiments with 47-mers, two experiments with 100-mers, three controls with no DNA, and two experiments with protamine-DNA complexes. A different tip was used for each experiment. In some of the experiments, multiple images were taken from one area. In other experiments, they were taken from more than one area.

A plot of the measured molecular lengths of the 22-mers, 47-mers and 100-mers (Figure 6) versus their known length in base pairs shows that all three molecules appear to have adopted the same conformation following their deposition on graphite in air. All three points fall along a straight line and the slope of this line, 0.247 nm per base pair, is very close to the expected axial rise per base pair for A form DNA.

Only one of the 86 pulses involving synthetic DNAs resulted in the attachment of structures not of the expected length. Forty total pulses were applied in negative control experiments (buffer + BAC). In five cases, linear structures were observed after pulsing, but the lengths were highly variable and did not cluster around any particular size.

Although additional structural detail appears to be obscured in many of the DNA images, the single-stranded four base sequence is clearly visible at both ends of the 47-mer (arrows, Figure 4B). Generally these single strands appear only as diffuse structures displaying little internal detail (see zoomed image, Figure 7A), possibly because the four base sequence is only loosely attached to the substrate.

Other features, such as the two separate phosphodiester chains and well defined major and minor grooves, are only visible in rare images. The image of one 47-mer that appears flattened against the graphite shows the two phosphodiester strands separated by what would appear to be the minor groove (Figure 7B). The distance measured across this groove (0.8-0.9 nm) is close to the 1.1 nm width expected for the wide and shallow minor groove in A form DNA (Conner *et al.*, 1982). Images such as those shown in Figures 8A and 8B are of high enough quality to also identify the direction of helical coiling. Three of the helical turns in this 47-mer are left-handed. Individual phosphodiester chains are also visible in the 100-mer (Figure 5C), but one of the grooves usually appears to be shallow and less pronounced. Such images represent the more typical level of resolution obtained with DNA imaged in air.

Complexes formed by the binding of bull protamine 1 to the 47-mer are extremely hydrophobic and attach readily to the graphite surface without pulsing. Images of several of these structures are shown in Figure 9. Although the width of the complex (3 nm) was measured to be only slightly larger than that of DNA, the lengths of the DNA molecules complexed with protamine were found to be substantially longer (16.5 ± 0.37 nm; $n = 8$) than the uncomplexed 47-mers. While the surfaces of most of the DNA-protamine complexes appear relatively featureless, five or six poorly defined bumps are generally visible along the length of the structure. Although they are less pronounced in the complex, the single-stranded ends still appear to be visible. However,

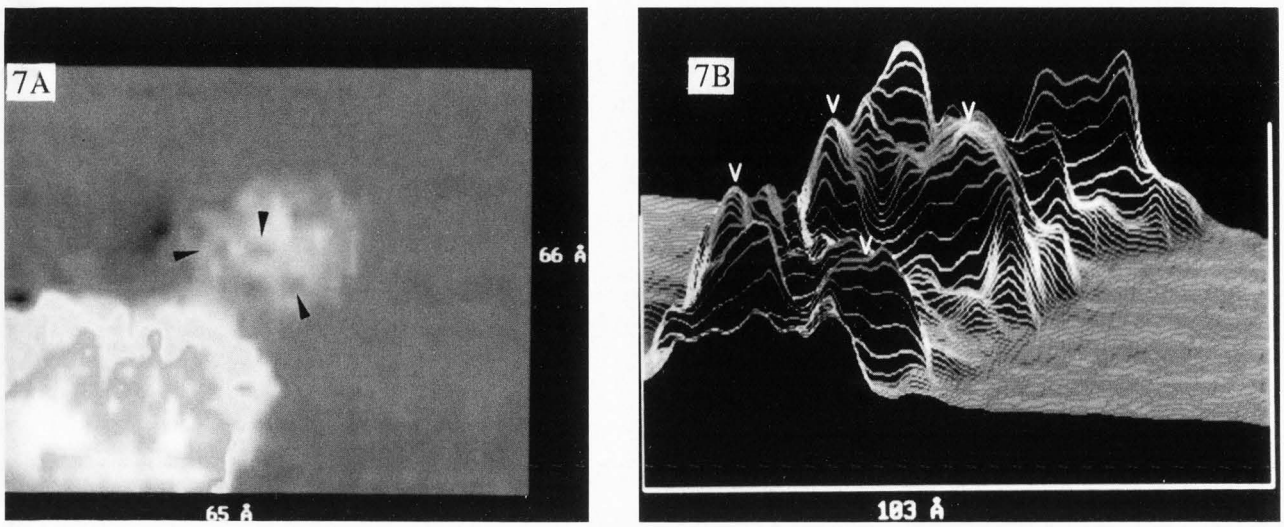

Figure 7. Other structural features resolved in 47-bp DNA molecules. **A.** An enlarged, unfiltered image of one of the single-stranded ends. Arrows point out material in the single-stranded region of the molecule. **B.** High magnification image of a 47-bp molecule showing the major and minor grooves. Arrows point out the individual phosphodiester strands.

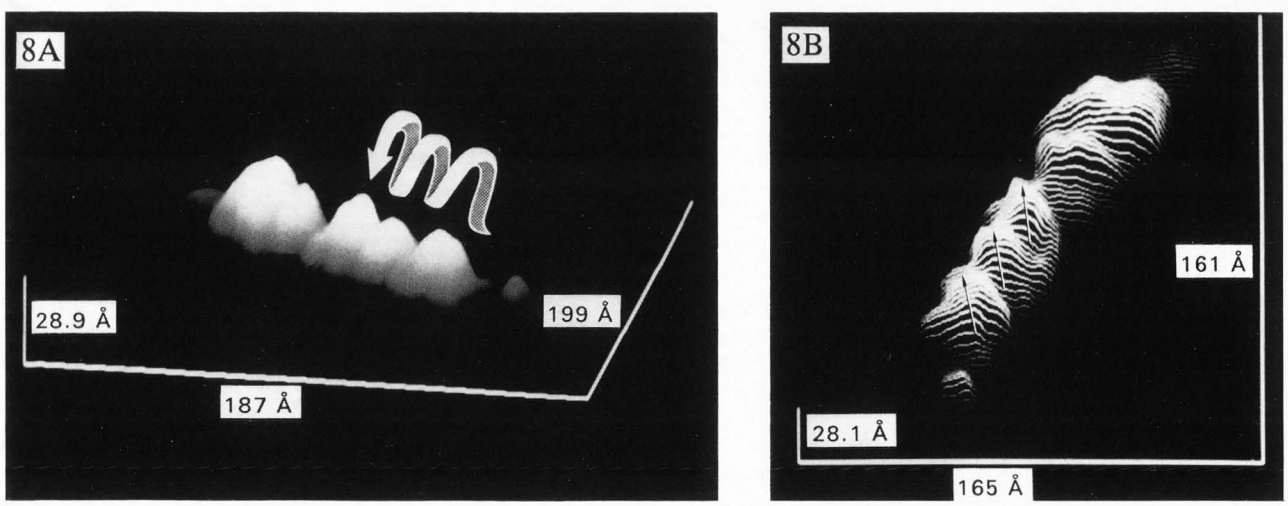

Figure 8. Images showing the direction of helical coiling in the 47-bp molecules. **A.** Five helical turns are apparent; the first three turns (from the right) are left-handed. The direction of coiling is not obvious in the last two turns. **B.** Different view of the same molecule showing direction of helical coiling (arrows) in first three turns.

neither the grooves nor the pronounced helical coiling characteristic of DNA are visible in any of the complexes after protamine binding. Only one very high resolution image (Figure 9C) revealed matched pairs of smaller bumps on the upper surface of the complex running in parallel along its length.

Discussion

The molecular lengths and helical periodicities measured for each of these synthetic DNAs suggest that all three molecules have adopted an A-like conformation, the preferred structure of DNA at low hydration

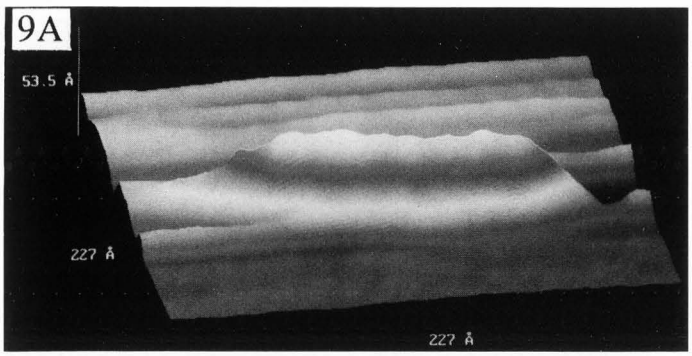

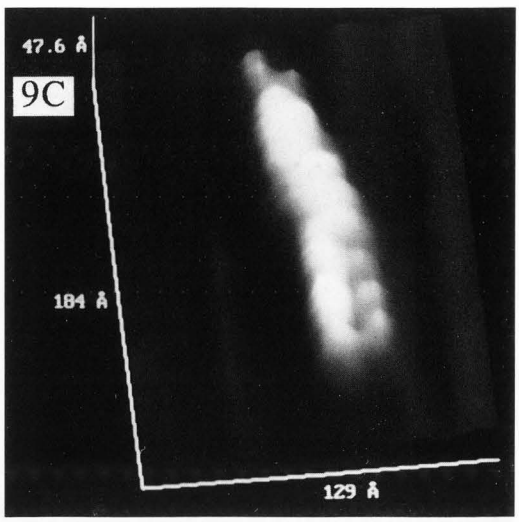

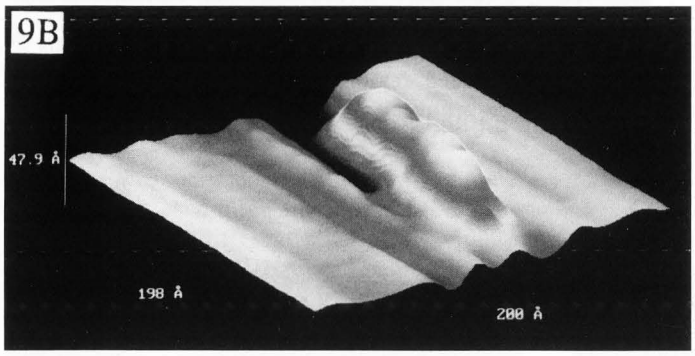

Figure 9. Complexes (A, B, and C) formed by the binding of bull protamine 1 to 47-bp DNA molecules. After air drying protamine on the surface of graphite (5 μl of protamine at 1.3 mg/ml in water), DNA was added (O.1 μl of DNA at 1.3 mg/ml in 10 mM sodium chloride) and the uncomplexed protamine was removed by rinsing with water. One highly resolved image (C) of a 47-mer complexed with protamine suggests that a series of regularly spaced "bumps" may be present on the upper surface of the complex.

levels when sodium is the counter ion (Saenger, 1984). Length measurements can be accurately determined to within a few tens of a nanometer with the STM. Since the A, B, D and Z forms of DNA differ significantly in inter-base-pair distance (0.256, 0.338, 0.303, and 0.371 nm respectively), the current results suggest that we should be able to identify conformational changes in stretches of DNA sequence as short as 10-bp. Such determinations provide evidence that tunneling microscopy can be used to obtain useful structural information about DNA and other macromolecules without actually achieving atomic resolution.

In the A conformation, the shallow major groove (0.28 nm deep) of DNA would be barely visible and the helical coiling of the two phosphodiester strands would only appear to be separated by the deep and narrow minor groove. Except on rare occasions, only one groove is visible in STM images of the duplexes. At least one-half of the mass of the DNA dried on the surface is contributed by tightly bound water molecules (this was determined by air-drying calf thymus DNA onto glass slides, scraping off the DNA, and quantitating the contribution of water to its mass by spectrophotometry at 260 nm). It seems reasonable, therefore, to expect that this water (as well as bound ions) might limit the visualization of at least one groove and obscure the separate phosphodiester strands.

Although left-handed non-Z conformers of DNA have never been confirmed by crystallographic data, their existence has been postulated for years based on stereochemical modeling (Gupta *et al.*, 1980; Olson, 1976; Sasisekharan and Pattabiraman, 1978). Images of the 47-mer obtained in this study provide the first experimental evidence that DNA molecules can adopt a left-handed, non-Z conformation. The possibility of electronic image inversion was ruled out by performing laser beam deflection experiments that determined the direction of tip movement and its relationship to helical sense or image "handedness". [The actual direction of tip movement during scanning (and its relationship to the "handedness" of imaged objects) was determined by very slowly rastering the tip in one direction while reflecting a laser beam off the surface of the piezo 24.4 meters down a dark hallway onto a wall. This allowed us to

magnify the beam sufficiently to determine its direction of movement, thereby identifying the direction of piezo movement and relating the direction of this movement to the raster direction observed during imaging]. This observation is further supported by our analyses of images obtained using the same STM and other DNAs. Only right-handed coiling has been observed in our previous images of calf thymus DNA (Beebe Jr. *et al.*, 1989) and biotinylated lambda DNA restriction fragments (unpublished data).

A close inspection of the Z-height variation between molecules shows that the apparent height of the imaged DNA is commonly less than 2 nm. Such measurements should not be used as an indicator of molecule or helix height. While measurements in the X and Y directions (width and length) are generally considered to reflect actual molecular dimensions, height information may be misleading since it must be determined relative to the graphite substrate which has a different electronic structure (and conductivity) than the DNA molecule. Height measurements are also affected by the compressibility of the molecule (due to the force exerted by the tip) and by environmental factors, including the extent of hydration and/or the degree of interaction between the molecule and substrate. Additionally, the helical structure of DNA may collapse or denature as a result of its strong interaction with the substrate surface. This distortion, as well as measurement errors induced by tip geometry or imperfections, suggest that molecular lengths (and to a lesser extent widths) may be the only dimensions in larger macromolecules that can be accurately assessed at the current time. Distortions in physical structure induced by association with the substrate would be expected to have less of an effect on a molecule's length than either its height or width.

How the BAC used to attach DNA to the tunneling tip prior to pulsing contributes to the STM images of DNA is presently unknown. Although it is clear that BAC and DNA in solution can interact to form stable, hydrophobic complexes (Delville *et al.*, 1986) at the air-liquid interface (Coetzee and Pretorius, 1979), nothing is known about how BAC interacts with DNA at the molecular level. The chemical structure of this molecule suggests that its benzene ring may interact with or intercalate between the bases of DNA. Other quaternary amines similar to BAC, such as the dodecyltrimethyl ammonium ion, interact weakly with the phosphodiester backbone of DNA through the quaternary amine while the alkyl groups strongly interact with each other facilitating a cooperative, hydrophobic binding (Delville *et al.*, 1986). It is tempting to speculate that the alkyl tails of BAC may provide the major attachment points which fix the DNA to the hydrophobic graphite substrate. It is more likely, however, that this detergent simply facilitates the binding of DNA to the tunnelling tip while the voltage pulse both desorbs the molecules from the tip and activates the carbon surface in a process similar to a glow discharge (Dubochet *et al.*, 1971).

Images of the 47-mer and 100-mer show that both molecules have one bulky end nearly twice the diameter and height expected for duplex DNA. Within these bulky regions, neither the individual phosphodiester strands nor the direction of helical coiling are resolved. A comparison of the base sequences of the 47-mer and 100-mer show that both DNAs contain an AT-rich region at one end. The length of the AT-rich sequence in the 47-mer matches closely the measured length of the bulky region. While it has not been demonstrated that BAC displays a base-sequence specificity in binding to DNA or that it remains bound to DNA after pulsing, it seems likely that the preferential binding of BAC molecules to the AT-rich regions of both DNAs may be responsible for the variability in diameter and height observed along the length of the molecule.

Using voltage pulses to apply these DNAs to graphite, two different types of deposition were observed. When the DNA was applied directly onto graphite and subsequently pulsed, individual unoriented molecules were usually found surrounding a centrally located mound of unidentifiable material. DNA molecules deposited in this manner provided the best high resolution images. Molecules deposited by pulsing after applying the DNA to the STM tip, on the other hand, were usually observed as arrays of individual filaments all oriented in the same direction. While it is unclear why the molecules within each group should be oriented by the pulse, the orientation was always observed to be linear (not radial) with respect to the tip. Differences in the structure and spacing of the molecules within the arrays and the presence of a single, well define "pit" in the surface produced by the pulse suggest that each structure represents a separate DNA molecule and not multiple images produced by a "multiple tip".

Measurements of DNA length obtained for 47-mers complexed with the arginine-rich bull protamine 1 molecule show that the binding of the protein to DNA prevents the change in DNA conformation from B to A that normally occurs upon DNA dehydration. The length of the complex appears to be representative of DNA length since we can see the single-stranded ends of the DNA molecules at the end of the complex. These results are consistent with infrared and other studies of nucleoprotamine that have previously suggested that protamine stabilizes DNA in the B-conformation (Bradbury *et al.*, 1962; Herskovits and Brahms, 1976; Sipski and Wagner, 1977; Suau and Subirana, 1977; Suwalsky and Traub, 1972). The measured widths of the complexes also appear to be consistent with the current idea that protamine molecules bind inside one of the grooves of DNA (Balhorn, 1982). The presence of the protamine molecules in the imaged complexes can contribute only 1 nm to the diameter of each DNA molecule at most.

Acknowledgements

This work was performed at the Lawrence Livermore National Laboratory under the auspices of the Department of Energy, contract #W-7405-ENG-48.

References

Allen MJ, Balooch M, Subbiah S, Tench RJ, Siekhaus W, Balhorn R. (1991). Scanning tunneling microscope images of adenine and thymine at atomic resolution. Scanning Microsc. **5**, 625-630.

Allison DP, Thompson JR, Jacobson KB, Warmack RJ, Ferrell TL. (1990). Scanning tunneling microscopy and spectroscopy of plasmid DNA. Scanning Microsc. **4**, 517-522.

Amrein M, Stasiak A, Gross H, Stoll E, Travaglini G. (1988). Scanning tunneling microscopy of recA-DNA complexes coated with a conducting film. Science **240**, 514-516.

Arscott PG, Lee G, Bloomfield VA, Evans DF. (1989). Scanning tunneling microscopy of Z-DNA. Nature **339**, 484-486.

Balhorn R. (1982). A model for the structure of chromatin in mammalian sperm. J. Cell Biol. **93**, 298-305.

Balhorn R, Gledhill BL, Wyrobek AJ. (1977). Mouse sperm chromatin proteins: quantitative isolation and partial characterization. Biochemistry **16**, 4074-4080.

Baro AM, Miranda R, Alaman J, Garcia N, Binnig G, Rohrer H, Gerber Ch, Carrascosa JL. (1985). Determination of surface topography of biological specimens at high resolution by scanning tunneling microscopy. Nature **315**, 253-254.

Barris B, Knipping U, Lindsay SM, Nagahara L, Thundat T. (1988). Images of DNA fragments in an aqueous environment by scanning tunneling microscopy. Biopolymers **27**, 1691-1696.

Beebe Jr TP, Wilson TE, Ogletree DF, Katz JE, Balhorn R, Salmeron MB, Siekhaus WJ. (1989). Direct observation of native DNA structures with the scanning tunneling microscope. Science **243**, 370-372.

Bendixen C, Besenbacher F, Laegsgaard E, Stensgaard I, Thomsen B, Westergaard O. (1990). Deoxyribonucleic acid structures visualized by scanning tunneling microscopy. J. Vac. Sci. Technol. **A8**, 703-705.

Beveridge TJ, Southam G, Jericho MH, Blackford BL. (1990). High-resolution topography of the S-layer sheath of the archaebacterium *Methanospirillum hungatei* provided by scanning tunneling microscopy. J. Bacteriol. **172**, 6589-6595.

Binnig G, Rohrer H. (1982). Scanning tunneling microscopy. Helv. Phys. Acta **55**, 726-735.

Binnig G, Rohrer H. (1985). The scanning tunneling microscope. Sci. American **253**, 50-56.

Blackford BL, Jericho MH, Mulhern PJ, Frame C, Southam G, Beveridge TJ. (1991). Scanning tunneling microscope imaging of hoops from the cell sheath of the bacteria *Methanospirillum hungatei* and atomic force microscope imaging of complete sheathes. J. Vac. Sci. Technol. **B9**, 1242-1247.

Bradbury EM, Price WC, Wilkinson GR. (1962). Polarized infrared studies of nucleoproteins, I: Nucleoprotamines. J. Mol. Biol. **4**, 39-49.

Chang H, Bard AJ. (1991). Observation and characterization by scanning tunneling microscopy of structures generated by cleaving highly oriented pyrolytic graphite. Langmuir **7**, 1143-1153.

Clemmer CR, Beebe Jr TP. (1991). Graphite. A mimic for DNA and other biomolecules in scanning tunneling microscope studies. Science **251**, 640-642.

Coetzee WF, Pretorius GHJ. (1979). Factors which influence the electron microscopic appearance of DNA when benzyldimethylalkylammonium chloride is used. J. Ultrastruct. Res. **67**, 33-39.

Conner BN, Takano T, Tanaka S, Itakura K, Dickerson RE. (1982). The molecular structure of d(CpCpGpG), a fragment of right-handed double-helical A DNA. Nature **295**, 294-299.

Cricenti A, Selci S, Chiarotti G, Amaldi F. (1991). Imaging of single-stranded DNA with the scanning tunneling microscope. J. Vac. Sci. Technol. **B9**, 1285-1287.

Cricenti A, Selci S, Felici AC, Generosi R, Gori E, Djaczenko W, Chiarotti G. (1989). Molecular structure of DNA by scanning tunneling microscopy. Science **245**, 1226-1227.

Dai JW, Jiao YK, Dong Q Su YX, Lin KC, He J, Shang GY, Yao JE. (1991). The surface structure of natural membrane of macrophages in water as studied by the scanning tunneling microscope. J. Vac. Sci. Technol. **B9**, 1184-1188.

Delville A, Laszlo P, Schyns R. (1986). Displacement of sodium ions by surfactant ions from DNA. A ^{23}Na-NMR investigation. Biophys. Chem. **24**, 121-133.

Driscoll RJ, Youngquist MG, Baldeschwieler JD. (1990). Atomic-scale imaging of DNA using scanning tunneling microscopy. Nature **346**, 294-296.

Dubochet J, Ducommun M, Zollinger M, Kellenberger E. (1971). A new preparation method for dark-field electron microscopy of biomacromolecules. J. Ultrastruct. Res. **35**, 147-167.

Dunlap DD, Bustamante C. (1990). Images of single-stranded nucleic acids by scanning tunneling microscopy. Nature **342**, 204-206.

Edstrom RD, Meinke MH, Yang X, Yang R, Evans DF. (1989). Direct observation of phosphorylase kinase and phosphorylase b by scanning tunneling microscopy. Biochemistry **28**, 4939-4942.

Eng L, Hidber HR, Rosenthaler L, Staufer U, Wiesendanger R, Guentherodt HJ, Tamm L. (1988). Summary abstract: Dipalmitoylphosphatidyl choline-Langmuir-Blodgett films on various substrates [Si(111), Au, Sn] studied by scanning tunneling microscopy. J. Vac. Sci. Technol. **A6**, 358-359.

Feng L, Andrade JD, Hu CZ. (1989). Scanning tunneling microscopy of proteins on graphite surfaces. Scanning Microsc. **3**, 399-410.

Foster JS, Frommer JE, Arnett PC. (1988). Molecular manipulation using a tunneling microscope. Nature **331**, 324-326.

Foster JS, Frommer JE. (1988). Imaging of liquid crystals using a tunneling microscope. Nature **333**, 542-545.

Gaczynska M, Chwialkowski M, Olejniczak W, Wojczuk S, Bartosz G. (1991). Scanning tunneling microscopy of human erythrocyte membranes. Biochem. Biophys. Res. Commun. **181**, 600-603.

Gimzewski K, Stoll E, Schlitter RR. (1987). Scanning tunneling microscopy of individual molecules of copper phthalocyanine adsorbed to polycrystalline silver surfaces. Surf. Sci. **181**, 267-277.

Gupta G, Bansal M, Sasiskharan V. (1980). Conformational flexibility of DNA: Polymorphism and handedness. Proc. Natl. Acad. Sci. USA **77**, 6486-6490.

Haggerty L, Watson BA, Barteau MA, Lenhoff AM. (1991). Ordered arrays of proteins on graphite observed by scanning tunneling microscopy. J. Vac. Sci. Technol. **B9**, 1219-1222.

Hameroff S, Simic-Krstic Y, Vernetti L, Lee YC, Sarid D, Wiedmann J, Elings V, Kjoller K, McCuskey R. (1990). Scanning tunneling microscopy of cytoskeletal proteins: Microtubules and intermediate filaments. J. Vac. Sci. Technol. **A8**, 687-691.

Hansma PK, Tersoff J. (1987). Scanning tunneling microscopy. J. Appl. Phys. **61**, R1-R23.

Hansma PK, Elings VB, Marti O, Bracker CE. (1988). Scanning tunneling microcopy and atomic force microscopy: Application to biology and technology. Science **242**, 209-216.

Heckl WM, Smith DPE, Binnig G, Klagges H, Hansch TW, Maddocks J. (1991). Two-dimensional ordering of the DNA base guanine observed by scanning tunneling microscopy. Proc. Natl. Acad. Sci. USA **88**, 8003-8005.

Herskovits TT, Brahms J. (1976). Structural investigations on DNA protamine complexes. Biopolymers **15**, 687-706.

Ito E, Takahashi T, Hama K, Yoshioka T, Mizutani W, Shimizu H, Ono M. (1991). An approach to imaging of living cell surface topography by scanning tunneling microscopy. Biochem. Biophys. Res. Commun. **177**, 636-643.

Keller RW, Dunlap DD, Bustamante C, Keller DJ, Garcia RG, Gray C, Maestre MF. (1990). Scanning tunneling microscopy images of metal-coated bacteriophages and uncoated, double-stranded DNA. J. Vac. Sci. Technol. **A8**, 706-712.

Keller D, Bustamante C, Keller RW. (1989). Imaging of single uncoated DNA molecules by scanning tunneling microscopy. Proc. Natl. Acad. Sci. USA **86**, 5356-5360.

Kim Y, Lieber CM. (1991). Scanning tunneling microscopy imaging of synthetic oligonucleotides and oligonucleotide-metal complexes. Scanning Microsc. **5**, 311-316.

Lang CA, Horber JKH, Hansch TW, Heckl WM, Mohwald H. (1988). Scanning tunneling microscopy of Langmuir-Blodgett films on graphite. J. Vac. Sci. Technol. **A6**, 368-370.

Lee G, Arscott PG, Bloomfield VA, Evans FE. (1989). Scanning tunneling microscopy of nucleic acids. Science **244**, 475-477.

Lesniewska E, Flamion PJ, Cachia C, Schreiber JP. (1991). Scanning tunneling microscopy of 16S ribosomal RNA in water. Biochem. Biophys. Res. Commun. **178**, 1280-1287.

Li MQ, Zhu J, Zhu JQ, Hu J, Gu MM, Xu YL, Zhang LP, Huang ZQ, Xu LZ, Yao XW. (1991). Direct observation of B-form and Z-form DNA by scanning tunneling microscopy. J. Vac. Sci. Technol. **B9**, 1298-1303.

Lindsay SM, Barris B. (1988). Imaging deoxyribose nucleic acid molecules on a metal surface under water by scanning tunneling microscopy. J. Vacuum Sci. Technol. **A6**, 544-547.

Lindsay SM, Thundat T, Nagahara L, Knipping U, Rill RL. (1989). Images of DNA double helix in water. Science **244**, 1063-1064.

Lu CD, Li MQ, Qui MY, Yao XW, Xu YL, Gu MM, Hu J. (1991). Conformation of DNA-DNA polymerase I complex observed by scanning tunneling microscopy. J. Biomol. Struct. Dynam. **9**, 233-238.

Mainsbridge B, Thundat T. (1991). Scanning tunneling microscopy of chloroplasts. J. Vac. Sci. Technol. **B9**, 1259-1262.

Mazrimas JA, Corzett M, Campos C, Balhorn R. (1986). A corrected primary sequence for bull protamine. Biochim. Biophys. Acta **872**, 11-15.

Miles MJ, Carr HJ, McMaster TC, I'Anson KJ, Belton PS, Morris VJ, Field JM, Shewry PR, Tatham AS. (1991). Scanning tunneling microscopy of a wheat storage protein reveals details of an unusual supersecondary structure. Proc. Natl. Acad. Sci. USA **88**, 68-71.

Miles MJ, McMaster T, Carr HJ, Tatham AS, Shewry PR, Field JM, Belton PS, Jeenes D, Hanley B, Whittam M, Cairns P, Morris VJ, Lambert N. (1990). Scanning tunneling microscopy of biomolecules. J. Vac. Sci. Technol. **A8**, 698-702.

Nakagiri N, Fujisaki H, Aizawa S. (1991). Scanning tunneling microscopy of bacterial flagella. J. Vac. Sci. Technol. **B9**, 1202-1205.

Olson WK. (1976). The spatial configuration of ordered polynucleotide chains. I. Helix formation and base stacking. Biopolymers **15**, 859-878.

Ohtani H, Wilson RJ, Chiang S, Mate CM. (1988). Scanning tunneling microscopy observations of benzene molecules on the Rh (111)-(3X3)(C_6H_6+2CO) surface. Phys. Rev. Lett. **60**, 2398.

Saenger W. (1984). Principles of Nucleic Acid Structure. Springer Verlag, New York, 368-384.

Salmeron M, Beebe T, Odriozola J, Wilson T, Ogletree DF, Siekhaus W. (1990) Imaging of biomolecules with the scanning tunneling microscope: Problems and prospects. J. Vac. Sci. Technol. **A8**, 635-641.

Sasisekharan V, Pattabiraman N. (1978). Structure of DNA predicted from stereochemistry of nucleoside derivatives. Nature **275**, 159-162.

Sipski ML, Wagner TE. (1977). The total structure and organization of chromosomal fibers in eutherian sperm nuclei. Biol. Reprod. **16**, 428-440.

Sleator T, Tycko R. (1988). Observation of individual organic molecules at a crystal surface by with the use of a scanning tunneling microscope. Phys. Rev. Lett. **60**, 1418-1421.

Smith DPE, Horber JKH, Binnig G, Nejoh H. (1990). Structure, registry and imaging mechanism of alkylcyanobiphenyl molecules by tunneling microscopy. Nature **344**, 641-644.

Smith DPE, Horber H, Gerber Ch, Binnig G. (1989). Smectic liquid crystal monolayers on graphite observed by scanning tunneling microscopy. Science **245**, 43-45.

Spong JK, Mizes HA, LaComb Jr LJ, Dovak MM, Frommer JE, Foster JS. (1989). Contrast mechanism for resolving organic molecules with tunneling microscopy. Nature **338**, 137-139.

Stemmer A, Reichelt R, Wyss R, Engel A. (1991). Biological structures imaged in a hybrid scanning transmission electron microscope and scanning tunneling microscope. Ultramicrosc. **35**, 255-264.

Suau P, Subirana JA. (1977). X-ray diffraction studies of nucleoprotamine structure. J. Mol. Biol. **117**, 909-926.

Suwalsky W, Traub W. (1972). An X-ray diffraction study of poly-L-arginine hydrochloride. Biopolymers **11**, 2223-2231.

Travaglini G, Rohrer H, Amrein M, Gross H. (1987). Scanning tunneling microscopy on biological matter. Surface Sci. **181**, 380-390.

Yang R, Evans DF, Christensen L, Hendrickson WA. (1990). Scanning tunneling microscopy evidence of semicrystalline and helical conducting polymer structures. J. Phys. Chem. **94**, 6117-6122.

Yeung KL, Wolf EE, Duman JG. (1991). A scanning tunneling microscopy study of an insect lipoprotein ice nucleator. J. Vac. Sci. Technol. **B9**, 1197-1201.

Youngquist MG, Driscoll RJ, Coley TR, Goddard WA, Baldeschwieler JD. (1991). Scanning tunneling microscopy of DNA: Atom-resolved imaging, general observations and possible contrast mechanism. J. Vac. Sci. Technol. **B9**, 1304-1308.

Zasadzinski JAN, Schneir J, Gurley J, Elings V, Hansma PK. (1988). Scanning tunneling microscopy of freeze-fracture replicas of biomembranes. Science **239**, 1013-1014.

Zheng NJ, Rau G, Hazlewood CF, Rau C. (1991). High-resolution, real-space imaging of conformational structures of poly-L-proline helixes. Scanning Microsc. **5**, 631-636.

Zhu XY, Poirier GE, White JM. (1991). Scanning tunneling microscopy of collagen molecules. J. Vac. Sci. Technol. **A9**, 179-181.

Discussion with Reviewers

J.K.H. Hörber: With pulses, a lot of uncontrollable events can happen: salt crystallization, deposition of tip material, even chemical reactions. In the case of graphite, this (may) possibly end up, specially at grain boundaries, with structures of the size typical for DNA, so that I would believe in such images only with a lot of statistical work.

Authors: We agree, and we did observe some of these effects of pulsing, including what appeared to be the deposition of tip material and the production of pits. But the material produced by pulsing on untreated graphite (after dipping the tip in buffer only) looked nothing like the structures we obtained when the tip was dipped in the various DNAs. The structures imaged after pulsing in the presence of the oligos were linear, not spherical bumps or domes. When we pulsed using a tip dipped in 22-mer, we obtained structures with similar lengths, averaging 5.5 nm long. When we pulsed using a tip dipped in 47-mer, we obtained linear structures with very similar lengths, averaging 11.6 nm long. When we used 100-mer, every pulse but one provided structures of similar length, averaging 21.5 nm. That one pulse produced an 8 nm structure. When we pulsed in the absence of DNAs, the structures deposited on the surface were rare and extremely variable in length and shape, ranging from 2 to 27 nm long. We collected images from eight **different** structures of each oligo (deposited in between two and four experiments) in an attempt to examine the statistics. A larger number was impractical because only 7% of the pulses resulted in the deposition of structures on the surface. But even with these few structures, the measured length of the object was consistent with the size of the oligo used.

J.K.H. Hörber: Since graphite can be so unfriendly for the DNA business, I would suggest to work on different substrates, for instance, freshly prepared crystalline gold surfaces, and try to omit the pulsing by other fixation methods.

Authors: While graphite can be "unfriendly", we know that all surfaces (including gold) have artifacts of one kind or another. In some experiments, the DNA was applied to the graphite (not the tip) and picked up as the surface was imaged with the tip prior to pulsing. In these experiments, we could search for a good area for imaging free of defects (such as grain boundaries), pulse the sample onto the surface, and begin the analysis knowing we were not in a region containing grain boundaries or other graphite artifacts. We also tried, briefly, to image molecules deposited onto gold surfaces without success.

D.P. Allison: Why not try to image a circular plasmid or some smaller circular molecules or a small DNA molecule complexed with an identifiable tag such as rhodium? If a 47-mer oligo can be immobilized on a protamine treated graphite surface and resist removal by the

scanning tip, why can't a more easily identifiable circular plasmid be imaged?

Authors: While we agree that circular DNAs would provide more convincing evidence that the DNA molecules are indeed DNA, linear oligos were used in this study because we needed to accurately measure the length of the oligos and use the lengths to determine the conformation of the molecules complexed with and without protamine. This could not be accomplished with circular or very long linear molecules because of the unique manner in which protamines package DNA. When protamine binds to small oligos at low oligo concentration, it appears to wrap around the helix and the linear structure appears to be retained. When protamine binds to linear or circular DNAs of significant length, however, the DNA molecule is coiled into a toroidal structure, much like you wind up a garden hose. When this happens, the number of loops in the coil cannot be determined (because they cannot be resolved) and consequently the length of the molecule cannot be measured. While we also agree that it would be best to use a DNA with an identifiable tag, the results that have been obtained with rhodium in our opinion are just as difficult to interpret. The 47-mer we used in this study was designed with a single-stranded four base sequence at both ends of the molecule for precisely that purpose. When looking for these oligos on graphite, the single-stranded ends provided additional support that the imaged structures were the DNA molecules we attached to the tip.

D.P. Allison: The authors make good arguments for their observations of helical periodicity, but there is nothing in the construction of their oligo to suggest a Z form or left-handed helix. What would CD (circular dichroism) spectroscopy of their 47-mer sample show?

Authors: While there is nothing in the sequence of the oligo to suggest a Z-form (and the length measurements suggest that it is not Z), the 3' half of the molecule is ~70% GC (guanine cytosine) rich. All we can suggest is that GC rich DNAs have been reported to have a propensity to adopt a left-handed helix. Unfortunately, we do not have enough of the oligo to consider a detailed analysis of its structure.

Circular dichroism is an extremely sensitive probe for conformation and it might prove useful in identifying whether or not part of the 47-mer exists in a left-handed helix, providing we could prepare enough sample and could obtain an appropriate standard of non-Z, left-handed DNA. This technique has proved most useful in identifying the structure of single stranded nucleic acids because the optical activity is derived from the stacking interactions of neighboring bases. Considerably less progress has been made in CD studies of double-stranded nucleic acids. Unfortunately, CD rarely provides absolute structural information; one must always make comparisons with standard structures that have been previously characterized by nuclear magnetic resonance (NMR) or X-ray analysis. A left-handed, B form of DNA is not, to our knowledge, available. Such a DNA has been predicted by computer modeling and CAP (catabolite gene activactor protein) binding studies (W. Saenger, Principles of Nucleic Acid Structure, Springer-Verlag, New York, 1984), but the only non-Z left-handed helical DNA that has been reported is poly (dl-dC)•poly (dl-dC) [Mitsui *et al.* (1970) Nature **228**, 1166]. Therefore, we chose not to focus our attention on proving that the 47-mer has a region of left-handed coiling, but we merely make an observation.

Reviewer IV: Bias pulses are said to cause reproducible surface modifications on HOPG under these conditions. How can the authors of this manuscript reconcile this body of literature with the claims made in the manuscript?

Authors: Conditions similar to those we have used here for depositing oligos onto graphite have been used by several groups to reproducibly modify the surfaces of graphite, Si, and GaAs (or related) surfaces. These include the production of pits as well as raised structures. In the studies on Si and GaAs, efforts were made to generate the smallest possible structures for lithography; and yet the smallest raised structures that could be produced were features 20 nm in width (Si) or 9 nm high (GaAs), features much larger than those reported in our study. Penner *et al.* (1991) performed pulse-induced nanolithography on graphite in water and organic liquids and showed that they could produce either pits or dome-shaped structures reproducibly. The diameter of these structures changed with the magnitude of the pulse voltage and varied from 0.7 to 50 nm. The structures were also round or dome-shaped and their diameter was shown to be highly dependent on the pulse voltage. Linear structures similar to those observed in this study were not detected. The objects observed by Penner *et al.* (1991) were, however, similar in shape and size to the amorphous structures we observed in our control pulses.

Reviewer IV: The issue of multiple tip images was not dealt with in sufficient depth. In their discussion, the authors incorrectly rule out the issue of multiple tip images based on two observations. "Subtle differences in the structure and spacing of the molecules", and re-imaging at higher resolution (smaller scan areas) does not rule out anything. I would suggest that Figures 4, 8 and possibly 9, are all "tip images" in which an array of asperities on the HOPG, possibly produced by the pulse, images the structure of the tip.

Authors: While we cannot rule out the possibility that the image in Figure 4A was produced by a multiple tip (these images were obtained using a non-commercial STM and the scan direction could not be changed), the objects imaged in Figures 4B, 8 and 9 were not generated by a multiple tip. These structures were imaged as isolated objects; they were not one of multiple objects imaged in the same area.

Reviewer IV: Whenever several closely spaced objects are lined up in the same direction (as they are in Figure

4), and when the details within each of those features are very similar (as they are in Figure 4), that is strong evidence that there are asperities on the surface imaging the tip structure.
Authors: We agree. We have, on at least one occasion, observed an array of objects that appeared remarkably similar in shape, suggesting that the objects (asperities) might be imaging the tip. But such images were uncommon. On objects with very little z-height, as in these structures (z-height 2 nm or less), the effect should not be observed frequently.

Reviewer IV: Careful examination shows that Figure 4B is a zoomed region of Figure 4A.
Authors: Figure 4B is not a zoomed region of Figure 4A. Figure 4B is a high-resolution image of a structure taken from a completely different experiment (preparation).

Reviewer IV: Why is it that the reported features are of the appropriate size for DNA?
Authors: The observation that the size of the objects corresponded to the length of oligo applied to the tip prior to pulsing in the majority of the experiments has convinced us that the objects **are** DNA molecules.

Reviewer IV: Were the reported sizes always observed?
Authors: No. Only in 8 out of 86 different pulse experiments using tips coated with DNA were deposited objects observed (other than the mound of material surrounding the pits). These were the objects measured in this study.

Reviewer IV: Were other sizes observed?
Authors: Yes. In one experiment with the 100-mers, an 8 nm structure was observed. Five objects were observed of variable length (3-27 nm) around the pit in 40 total pulses applied in the negative control experiments.

Reviewer IV: How often was nothing observed?
Authors: No deposited objects were observed in 78 of the 86 pulses using tips coated with DNA.

Reviewer IV: Was something similar ever observed when no pulse was used?
Authors: No.

Reviewer IV: A surface sensitive spectroscopy, such as XPS or Auger, might be able to detect the presence of pulsed on molecules if enough were deposited. The DNA could also be radio-labeled and detected in this way. Were these experiments tried? Was there an attempt to reproduce these results on another surface?
Authors: Two few oligos appear to be deposited per pulse (usually less than 10) for us to consider X-ray photoelectron spectroscopy (XPS) or Auger. We did end-label DNA with ^{32}P and found that radio-label was bound to the surface after pulsing. But this result was not described because it only says that DNA is attached somewhere on the graphite surface. It would not help us prove that the imaged structures are oligonucleotides. It is likely that considerable DNA may be deposited in the unidentifiable ring of material that surrounds the pits generated by the pulse. No, we did not attempt to pulse deposit the material onto other types of surfaces.

Reviewer IV: The authors do not seem to have considered the effect of the tip shape on the apparent width of the DNA-protamine complexes. Indeed it seems like the measured widths are too narrow to actually be DNA.
Authors: The measured width of the protamine-DNA complex, 3 nm, is 50% larger than the diameter of DNA. This difference could be due to two effects: **a)** an increase in diameter produced by protamine binding (computer models suggest the diameter of the complex should be between 2.5 and 3 nm), or **b)** a distortion in lateral measurement made by the effect of the tip shape. The observed measurement may represent a combination of both effects. STM images of the RecA-DNA complex show only a slight increase in complex diameter (12 nm measured versus 10 nm expected) over that expected. The oligos imaged in this study also have a diameter of approximately 2.4 nm. In both of these studies, the observed diameter of the structures are approximately 20% larger than expected. This could be explained if **a)** the tip were to have a slight effect on the diameter measurements, or **b)** the molecules were to flatten slightly against the surface as they dry. Both possibilities could be correct, and we cannot (using the current data) discriminate between them.